T-Cell Activation by Soluble MHC Oligomers Can Be Described by a Two-Parameter Binding Model

Jennifer D. Stone, Jennifer R. Cochran, and Lawrence J. Stern
Department of Chemistry, Massachusetts Institute of Technology, Cambridge, Massachusetts 02139 USA

ABSTRACT T-cell activation is essential for initiation and control of immune system function. T cells are activated by interaction of cell-surface antigen receptors with major histocompatibility complex (MHC) proteins on the surface of other cells. Studies using soluble oligomers of MHC–peptide complexes and other types of receptor cross-linking agents have supported an activation mechanism that involves T cell receptor clustering. Receptor clustering induced by incubation of T cells with MHC–peptide oligomers leads to the induction of T-cell activation processes, including downregulation of engaged receptors and upregulation of the cell-surface proteins CD69 and CD25. Dose–response curves for these T-cell activation markers are bell-shaped, with different maxima and midpoints, depending on the valency of the soluble oligomer used. In this study, we have analyzed the activation behavior using a mathematical model that describes the binding of multivalent ligands to cell-surface receptors. We show that a simple equilibrium binding model accurately describes the activation data for $CD4^+$ T cells treated with MHC–peptide oligomers of varying valency. The model can be used to predict activation and binding behavior for T cells and MHC oligomers with different properties.

INTRODUCTION

In recognition of and response to foreign antigens, $CD4^+$ T cells have an important role in the immune system. $CD4^+$ T-cell activation is triggered upon specific interaction of T-cell surface receptors (TCR) with foreign antigens bound to class II major histocompatibility complex (MHC) proteins found on the surface of B cells, macrophages, and other antigen-presenting cells (Germain, 1994; Davis et al., 1998). MHC-TCR engagement triggers a cascade of signaling events, including phosphorylation of receptor subunits, docking of receptor-associated signaling and adapter proteins, activation of cytoplasmic signaling cascades, and up-regulation of several gene products (Cantrell, 1996; Qian and Weiss, 1997). The complete activation program also requires participation of antigen-independent adhesion and costimulatory molecules from both the T cell and antigen-presenting cell (Chambers, 2001), which can lead to formation of cell-surface supramolecular activating clusters or "immune synapses" (van der Merwe et al., 2000), and eventually cytokine secretion, clonal proliferation, and induction of other T-cell effector functions required to help clear the foreign antigen from the host.

The precise molecular events that induce T-cell triggering upon TCR ligation are not well understood, but substantial evidence points to receptor clustering as an important component of the signaling in this system (Germain, 1997). Early studies showed that antibody-mediated clustering of TCR (Janeway, 1995), or clustering of chimeric TCR cytoplasmic domains (Irving and Weiss, 1991; Letourneur and Klausner, 1991) could trigger T-cell activation processes. More recently, soluble MHC–peptide oligomers have been used as reagents to investigate T-cell activation processes (reviewed in Cochran et al., 2001a). These reagents include antibody-linked MHC dimers (Abastado et al., 1995), dimers created through chimeric fusions of MHC-peptide complexes to antibody Fc domains (Casares et al., 1999; Appel et al., 2000; Hamad et al., 1998), streptavidin-linked oligomers of biotinylated MHC-peptide complexes (Boniface et al., 1998; Crawford et al., 1998), and a series of chemically-defined MHC dimers, trimers, and tetramers prepared using flexible peptide-based cross-linkers (Cochran and Stern, 2000). These studies demonstrated that multivalent TCR engagement is necessary for $CD4^+$ T-cell triggering, with an MHC dimer as the minimal activating unit (Cochran et al., 2000; Boniface et al., 1998). T-cell activation induced by such soluble oligomeric reagents exhibits nonsaturating, bell-shaped dose–response curves (Cochran et al., 2000), but these activation relationships have not been related to binding constants or other molecular properties of the system. Moreover, fluorescent MHC oligomers increasingly are used to track antigen-specific T-cell populations in clinical samples (Ferlin et al., 2000; McMichael and O'Callaghan, 1998), and understanding the correlation between binding levels and molecular properties such as MHC–TCR affinity or TCR clustering is urgently needed.

To gain insight into the binding behavior of MHC oligomers, and the relationship between MHC–TCR binding and the resultant activation response, we have applied a simple receptor cross-linking model developed originally for characterization of equilibrium binding of multivalent ligands to receptors on mast cells (Perelson, 1981). Here, we show that the model accurately describes the behavior of soluble MHC oligomers in inducing activation processes in T cells for a variety of oligomer valencies, MHC–TCR

Received for publication 9 May 2001 and in final form 27 July 2001.

Address reprint requests to Lawrence J. Stern, Dept. of Chemistry, Massachusetts Institute of Technology, 77 Massachusetts Ave., Cambridge, MA 02139. Tel.: 617-253-2849; Fax: 617-258-7847; E-mail: stern@mit.edu.

0006-3495/01/11/2547/11 $2.00

affinities, and cross-linking strategies. The striking correlation of the model with the experimental data in this system shows that several T-cell responses are directly related to the number of multivalently engaged receptors. The behavior of the model under different experimental conditions suggests possible mechanisms for the cellular regulation of antigen sensitivity in T cells.

MATERIALS AND METHODS

Preparation of class II MHC–peptide oligomers

HLA-DR1 α and β extracellular domains (Cochran and Stern, 2000) were expressed in *Escherichia coli* cells as inclusion bodies, solubilized in 8 M urea, purified by ion exchange, and refolded by dilution of the denaturant under redox-controlled conditions in the presence of peptide, as previously described (Frayser et al., 1999). Cysteine residues introduced into the α or β subunit C-termini (α_{cys}, β_{cys}, α_{Lcys}, and β_{Lcys}) were used for cross-linking. In some experiments, the cysteine was introduced immediately after the membrane proximal immunoglobulin domain (α_{cys}, β_{cys}); in others, the 5–10-residue connecting-peptide region was included before the cysteine (α_{Lcys}, β_{Lcys}). Antigenic peptide Ha[306–318] (PKYVKQNTLKLAT) derived from influenza hemagglutinin (Lamb et al., 1982), control peptide A2[103–117] (VGSDWRFLRGYKQYA) (Chicz et al., 1992), and cross-linkers X3X (fβEK′SGSK′G) and X14X (fβEK′SGSGESGSEGSSEGK′G) (Cochran et al., 2001b) and related trivalent and tetravalent peptide-based cross-linkers (Cochran and Stern, 2000), where fβ is fluoresceinyl-β-alanine and K′ is $N(\epsilon)$aminocaproylbenzylmaleimide lysine, were synthesized using 9-fluorenylmethoxycarbonyl (FMOC) chemistry, purified by reverse-phase high-performance liquid chromatography, and verified using mass spectrometry. The refolded HLA-DR1–peptide complexes carrying a cysteine on either the α or β subunit were oligomerized by reaction of the introduced thiols with maleimidyl groups on the peptide-based cross-linkers. Cross-linker was added in small aliquots to freshly-reduced MHC protein at room temperature over a period of five hours to a final molar ratio of MHC:cross-linker of 2:1 for dimers, 3:1 for trimers, and 4:1 for tetramers (Cochran and Stern, 2000). Purified MHC–peptide oligomers were isolated using two Superdex 200 HR 10/30 columns (Pharmacia, Peapack, NJ) in series, and further characterized by SDS-PAGE (Cochran and Stern, 2000). For binding assays, fluorescent MHC–peptide monomers were prepared by reaction of the HLA-DR1-introduced cysteine residue with fluorescein-malemide (Pierce, Rockford, IL) followed by purification by gel filtration chromatography (Cochran and Stern, 2000).

T-cell activation and binding assays

The T-cell clone HA1.7 (Lamb et al., 1982) used in many of the experiments presented herein is specific for the Ha peptide bound to HLA-DR1, and was maintained by biweekly stimulation with peptide-pulsed irradiated antigen-presenting cells and rested seven days before activation assays (Cochran et al., 2000). Two HLA-DR1-restricted, Ha-peptide specific, T-cell clones, Cl-1 (Sette et al., 1994) and HaCOH8 (gift of Corrine Moulon, Warner-Lambert, Paris), and a short-term polyclonal T-cell line, HA03 (Cameron et al., 2001), were maintained similarly. T-cell activation assays were performed as previously described (Cochran et al., 2000). Briefly, MHC–peptide oligomers were added to 7.5×10^4 T cells in round-bottom 96-well plates and incubated at 37°C, 7% CO_2. After the desired incubation time, cells were placed on ice and stained concurrently with fluorescent monoclonal antibodies against T cell surface markers: R-phycoerythrin (PE)-labeled anti-CD3 (UCHT-1) and allophycocyanin (APC)-labeled anti-CD69 (FN50) or APC-anti-CD25 (M-A251) (all from Pharmingen, San Diego, CA). Cells were washed with phosphate-buffered saline (1 mM KH_2PO_4, 10 mM Na_2HPO_4, 137 mM NaCl, 3 mM KCl, pH 7.4) containing 1% fetal bovine serum and 0.1% sodium azide and analyzed by flow cytometry. Fluorescence data were obtained with a Becton-Dickinson FACS Calibur flow cytometer and analyzed using Cell Quest software. The number of MHC–peptide complexes bound during the course of the T-cell activation assay was measured simultaneously with T-cell activation markers using the fluorescein molecules incorporated into the cross-linkers and multicolor flow cytometry (Cochran et al., 2000). The number of CD3 molecules downregulated upon oligomer treatment, and the number of MHC–peptide complexes bound per cell, were converted from mean fluorescence using SPHERO Rainbow calibration particles (Spherotech, Libertyville, IL) containing known amounts of PE and fluorescein equivalents.

Generation of calculated cross-linking and binding curves

For a given K_X, K_D, and R_{tot}, the implicit equation for R_{eq} (see Eqs. 1 and 2 below) was solved numerically for each valency of oligomer and each concentration using the secant method (Kreyszig, 1993). That value was then used to calculate the number of oligomers bound per cell with each possible valency. The calculations were performed using programs created in FORTRAN 77 and MAPLE V. Φ_{xlink}, R_{multi}, R_{dimer}, and L_{bound} were calculated from binding distributions as described in the Model section of this paper.

Fitting experimental activation and binding data

Fits of the model to the experimental sets were solved by a three-parameter minimization of K_X, K_D, and scale factor, using known R_{tot}. Minimization reduced the total χ^2 by iterative testing of combinations of parameter values one interval above and below the current values of K_D, K_X, and scale factor, and adopting the combination with the lowest χ^2 as the new values. The interval was reduced until convergence. A wide range of initial guesses was tried for each data set to ensure uniqueness of the fit parameters. The uncertainty for each parameter, δ^2_{aj}, was determined by

$$\delta^2_{aj} = \frac{2}{(N-n)(\chi^2_{p+\sigma} - 2\chi^2_p + \chi^2_{p-\sigma})},$$

where N is the number of measurements used for the fit, n is the number of parameters being fit by the program, and the χ^2 values correspond to the values calculated with the parameter p varying about the best fit value by the interval σ (Bevington, 1969).

MODEL

Distribution of bound states for a multivalent ligand of a cell-surface receptor

A simple equilibrium model that describes the interaction of multivalent ligands with cell-surface receptors was used to simulate activation dose–response curves. Binding and cross-linking parameters were obtained by least-squares fitting of curves to experimental binding and activation data. This model was originally developed to describe general receptor binding by multivalent ligands, and has been applied to the release of histamine from basophils (Perelson, 1981), a response that requires receptor cross-linking (DeLisi and Siraganian, 1979). Similar models have been used to fit data for IgE-Fcϵ receptor clustering (Hlavacek et al., 1999), dissociation of insulin and nerve growth factor from their cross-linked receptors (DeLisi and Chabay, 1979), viral attachment to cell-surface receptors (Wickham et al., 1990), and dimeric MHC–peptide complexes binding to $CD8^+$ T cells (Fahmy et al., 2001).

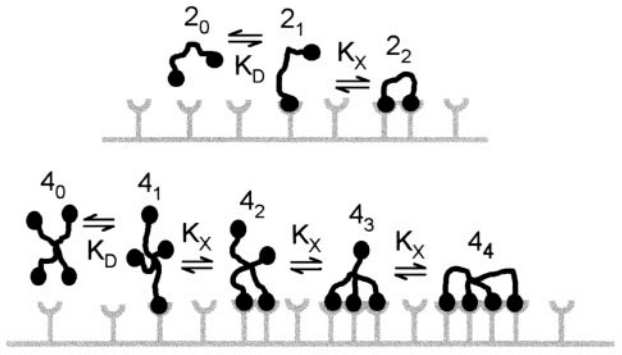

FIGURE 1 Schematic description of oligomer binding for a dimer (*top*) and a tetramer (*bottom*). The top row shows a dimer binding sequentially to monomeric cell surface receptors. The terminology for the binding state is shown above each oligomer. The bottom panels show the same scheme for a tetramer binding sequentially to monomeric cell surface receptors.

The model describes the distribution of different bound states of a multivalent ligand interacting with a monovalent receptor (Fig. 1). For example, a ligand dimer may be bound monovalently (2_1) or divalently (2_2), assuming that both ligand units can bind simultaneously, or it may not be bound at all (2_0, Fig. 1, *top*). Similar states can be described for a ligand tetramer (Fig. 1, *bottom*). The model can be used to describe the relative amounts of these states under different conditions. The monovalent binding of a ligand to its receptor is characterized by the equilibrium dissociation constant K_D (units of molarity). The tendency for multivalent binding is assigned to the cross-linking constant K_X (units of $(\#/\text{cell})^{-1}$), with the assumption that binding of each additional monomer within the oligomer is described by the same constant. The actual independent modeling parameter is κ, the unitless product of the receptor density (R_{tot}/A, units of $(\text{area})^{-1}$, where A is the surface area of the cell) and a 2-dimensional equilibrium-binding constant ($K_X * A$, units of area). Because the receptor density is less convenient to measure experimentally than the number of receptors per cell, we report the cross-linking constant $K_X = \kappa/R_{tot}$. The model also assumes that rapid binding equilibrium is attained, and that the free ligand concentration is not significantly depleted by binding to cell surface receptors. At the cell densities conventionally used in these experiments ($1–5 \times 10^6$ cells/mL), ligand is not significantly depleted for ligand concentrations greater than 10^{-10} M, even at 100% receptor occupancy.

Calculation over a range of concentrations yields the distinctive distribution of the various bound states, which is sensitive to changes in K_D, K_X, and the total receptor number (R_{tot}). At equilibrium, the amount of oligomer with valency (v) that is bound using i ligands can be found by (Perelson, 1981)

$$\nu_{i,eq} = \frac{v!}{i!\,(v-i)!}\,(K_X)^{i-1}\,\frac{L_0}{K_D}\,(R_{eq})^{i}, \qquad (1)$$

where $\nu_{i,eq}$ is the number of oligomers of valency v bound i times per cell at equilibrium, L_0 is the bulk concentration of oligomer, and R_{eq} is the number of unbound receptors per cell at equilibrium. The value of R_{eq} must be found from the numerical solution of

$$R_{tot} = R_{eq}\left(1 + v\,\frac{L_0}{K_D}\,(1 + K_X R_{eq})^{v-1}\right), \qquad (2)$$

and R_{bound} is found by

$$R_{bound} = R_{tot} - R_{eq}. \qquad (3)$$

Several related parameters describing the system can be extracted from this type of calculation. For example, the number of cross-links (Φ_{xlink}) formed by oligomers bound multivalently can be calculated as

$$\Phi_{xlink} = \sum_{i=2}^{v} (i-1)\nu_{i,eq}. \qquad (4)$$

This is the original measure that was used in previous studies (Perelson, 1981; Hlavacek et al., 1999). A tetramer bound divalently is considered to have one cross-link, whereas one bound trivalently has two cross-links. In addition, the number of cross-linked receptors (R_{multi}), i.e., those associated with oligomers bound multivalently, can be found by

$$R_{multi} = \sum_{i=2}^{v} i\nu_{i,eq}. \qquad (5)$$

The number of discrete receptor dimers per cell (R_{dimer}) can be found using

$$R_{dimer} = \sum_{i=2,4,6,\ldots}^{v} \frac{i}{2}\,\nu_{i,eq}. \qquad (6)$$

A tetramer bound tetravalently forms two discrete receptor dimers, whereas one bound trivalently forms only one. Finally, the total number of oligomers bound per cell (L_{bound}) can be calculated using

$$L_{bound} = \sum_{i=1}^{v} \nu_{i,eq}. \qquad (7)$$

Theoretical distribution curves

The predicted distribution of bound states as a function of concentration for fixed K_X, K_D, and R_{tot} values is shown for a dimeric ligand in Fig. 2, *A*, *B*, and *C*, and for a tetrameric ligand in Fig. 2, *D*, *E*, and *F*. The plots in Fig. 2 were calculated using the same R_{tot} (24,000 per cell) and K_D (1.4 μM) values, but with three different values for K_X. When the cross-linking tendency (K_X) is low (2.0×10^{-5} per cell^{-1}), as in Fig. 2, *A* and *D*, the fraction of oligomers bound multivalently (using two, three, or four ligands) is low. The number of ligands bound monovalently rises rapidly to saturation with increasing ligand concentration. In the tetramer plot (Fig. 2 *D*), the dashed line representing the sum of ligands bound multivalently (R_{multi}) is similar to the symmetric plot of divalently bound tetramers (4_2), because few or no trivalently (4_3) or tetravalently (4_4) bound oligomers are present. When the tendency to cross-link (K_X) is ten-fold higher, as in Fig. 2, *B* and *E*, significant amounts of di-, tri-, and tetramerically bound ligands accumulate at intermediate concentrations, and decrease at higher concentrations. The decrease at high concentrations can be understood by considering that mass action drives the formation of monovalently bound oligomers at high concentrations of ligand. In the tetramer plot (Fig. 2 *E*, *solid line*), the curve describing the total number ligands bound multivalently (R_{multi}) begins to show some discernible asymmetry with a shallower slope at low ligand concentration and a sharper slope at high concentration. In Fig. 2, *C* and *F*, the cross-linking tendency (K_X) is again raised by 10-fold, and the asymmetry of the multivalently bound curve in Fig. 2 *F* is even more pronounced. The curves representing oligomers bound with their maximum valency rise rapidly with concentration. These oligomers remain maximally bound with increasing concentration, and are only slowly replaced by oligomers bound with lower valency, and then by monovelently bound oligomers. The curve describing monovalently bound oligomer rises at an even higher concentration than for lower K_X, because it is even more difficult for a monovalent interaction to compete with multivalent interactions of bound oligomers.

The effect of varying parameters other than K_X also can be determined. If the K_D is reduced by a factor of ten, the result is a linear shift of the curves to lower concentrations. Increasing K_D shifts the curves in the opposite direction. Alternatively, if R_{tot} is changed ten-fold, an identical

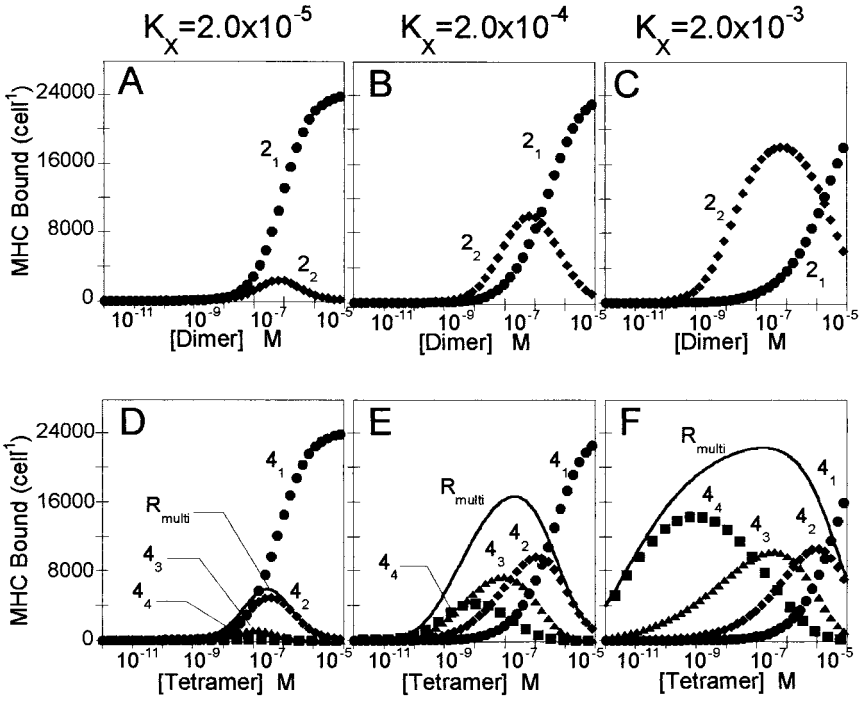

FIGURE 2 Binding distribution plots. The distribution of variously bound oligomers as a function of oligomer concentration is shown in terms of the number of MHC molecules bound. (*A–C*) The behavior of a dimeric ligand binding to monovalent cell surface receptors as the cross-linking capacity K_X increases in each panel as shown above the plots. (*D–F*) The behavior of a tetrameric ligand binding to monovalent cell surface receptors. Oligomers bound monomerically (●), dimerically (♦), trimerically (▲), and tetramerically (■), are shown. The solid line on the tetramer plots *D–F* represents the sum of the multivalently bound oligomers, R_{multi}.

effect on the shape of the curves is observed as for the corresponding change in K_X; however, the height of the curve will be scaled to correspond to the increased number of receptors per cell.

RESULTS

Analysis of experimental dose–response curves for activation of a T cell clone by a series of MHC oligomers

To investigate the molecular triggering mechanism of T-cell activation, we have previously developed a series of chemically-defined MHC–peptide oligomers of the human class II protein HLA-DR1 (Cochran and Stern, 2000) and used these to trigger activation processes in the well-characterized, influenza-specific human T-cell clone HA1.7 (Lamb et al., 1982). This series of MHC dimers, trimers, and tetramers was prepared using synthetic peptide-based cross-linking reagents that were designed to be flexible and to allow simultaneous binding of multiple MHC molecules to the T-cell surface. Activation processes induced by these oligomers were measured as changes in cell surface expression of activation markers detected by multicolor flow cytometry. The dose–response of T-cell activation induced by MHC dimers, trimers, and tetramers was measured for three activation markers: downregulation of T-cell receptor subunits (CD3) (Valitutti et al., 1997), upregulation of a T-cell-associated lectin-like protein conventionally used as an early T-cell activation marker (CD69) (Testi et al., 1994), and upregulation of the interleukin-2 receptor α subunit involved in the autocrine proliferative response (CD25) (Waldmann, 1989). The dose–response for T-cell activation triggered by each of the oligomers displayed a bell-shaped curve (Cochran et al., 2000) similar to those predicted by the simple equilibrium binding model. Increasing oligomer size caused a shift in the activation maximum to lower concentration and an increase in the maximum amplitude, behavior characteristic of the model applied here (Perelson, 1981).

The dose–response curves were fit using the model described above, using an experimentally determined value (24,000) for R_{tot}, the number of receptors per untreated T cell. Figure 3 shows the fits of the predicted R_{multi} values to experimental data for CD3 downregulation in the HA1.7 T cell clone (Cochran et al., 2000) measured at 12 and 27 h, respectively, after addition of MHC oligomers to the T cell culture. Filled symbols indicate the experimental data (*diamonds*, dimers; *triangles*, trimers; *squares*, tetramers), and smooth curves represent the predicted number of TCR multivalently bound (R_{multi}) using best-fit values for K_D, K_X, and a scale factor relating R_{multi} to the experimental measure

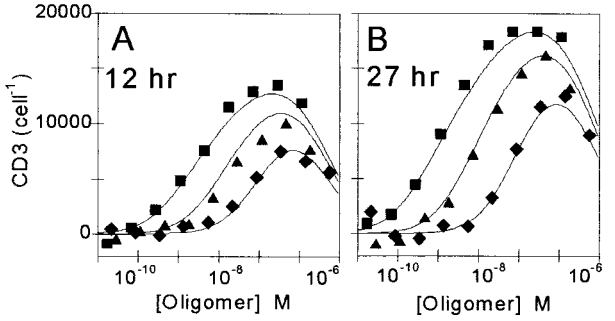

FIGURE 3 Comparison of experimental CD3 downregulation data and model predictions. The predicted sum of multivalently bound oligomers at each concentration was fit to experimental CD3 downregulation data for treatment with a dimer (♦), trimer (▲), and tetramer (■) (Cochran et al., 2000). (*A*) The response of HA1.7 T cells at 12 h of incubation with the oligomers. (*B*) The response at 27 h of incubation with the oligomers. Best fit parameters shown in Table 1.

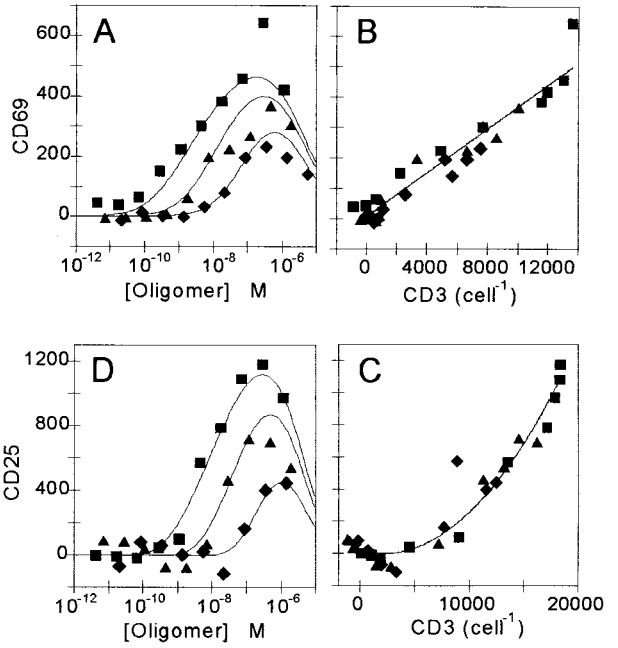

FIGURE 4 (*A*, *B*) CD69 and (*C*, *D*) CD25 upregulation data and model predictions for a T cell clone. (*A*) The predicted sum of multivalently bound oligomers at each concentration was fit to experimental HA1.7 CD69 upregulation data for treatment with a dimer (♦), trimer (▲), and tetramer (■) (Cochran et al., 2000). (*B*) The relationship between CD69 and CD3 responses with a best fit line. The linear relationship suggests that a single scale factor could be used to relate CD69 response to R_{multi}. (*C*) The relationship between CD3 and CD25 responses with a best-fit quadratic curve. The curved relationship suggests that CD25 response is not directly related to R_{multi}, and a quadratic filter was used to relate the model predictions to the data. (*D*) The experimental HA1.7 CD25 response to the dimer (♦), trimer (▲), and tetramer (■) treatments fit using a quadratic filter based on the relationship in (C). Parameters for the fits are shown in Table 1.

of internalized TCR. The curves obtained from a single experiment with different oligomers were fit simultaneously. The predicted curves fit well to the experimental data to within the expected uncertainty of the measurements. Best-fit parameters for data collected at different times after oligomer addition are similar: $K_D = 1.4 \pm 0.1$ μM (12 hr) or $K_D = 1.7 \pm 0.4$ μM (27 hr), and $K_X = 1.92 \pm 0.05 \times 10^{-4}$ per cell^{-1} (12 hr) or $K_X = 3.15 \pm 0.01 \times 10^{-4}$ per cell^{-1} (27 hr) (Table 1). The scale factor relating the predicted number of multivalently-engaged receptors to the experimental number of downregulated receptors was 0.776 ± 0.001 at 12 hr and 0.996 ± 0.001 at 27 hr. The value of the scale factor approaches one at long incubations, indicating that all engaged receptors eventually become downregulated as part of the T-cell activation program, as suggested by cellular studies (Valitutti et al., 1997; Germain, 1997). The extracted values for K_D are within the range of affinities reported for other class II MHC-TCR systems determined by direct binding measurements using soluble receptors and ligands (Davis et al., 1998). The extracted values for K_X, and for the dimensionless value $\kappa = K_X * R_{tot}$, are comparable to those observed in other systems (Hlavacek et al., 1999; Wickham et al., 1990; Fahmy et al., 2001). For example, the K_X determined for IgE-Fcϵ receptor cross-linking by multivalent antigen was 1.35×10^{-5} per cell^{-1} (Hlavacek et al., 1999), and for the attachment of adenovirus to HeLa cells, a K_X of 5×10^{-3} per cell^{-1} was calculated (Wickham et al., 1990). These values correspond to κ values of 13 and 30, respectively. The κ values determined for binding of class I MHC-IgG fusion proteins to CD8$^+$ T cells range from 1 to 73 for cells in different activation states (Fahmy et al., 2001). Our values of $\kappa = 4-8$ are within the range observed in these systems.

TABLE 1 Binding and cross-linking parameters for several experimental markers of T-cell activation for the clone HA1.7*

Experiment	K_D (μM)	K_X ($\times 10^{-4}$ cell)
CD3 (12 hrs)	1.40 (0.12)	1.92 (0.05)
CD3 (27 hrs)	1.70 (0.40)	3.15 (0.01)
CD69 (12 hrs)	1.40 (0.60)	2.30 (0.60)
CD25 (27 hrs)†	1.80 (0.30)	3.00 (0.01)
Direct Binding	1.60 (0.30)	0.95 (0.01)

*R_{tot} was measured at 24,000 in these experiments, MHCs were linked through β subunit cysteines (β_{Lcys}) using peptide-based cross-linkers (Cochran et al., 2000). Values in parentheses represent parameter uncertainties from the least squares fit (see Methods).

†CD25 upregulation was fit with this scale:

$$CD25 = 4 \times 10^{-5} \times (R_{multi})^2 - 0.0073 \times R_{multi}.$$

Activation of HA1.7 T cells measured using other markers could also be described by the model. Upregulation of the early activation marker CD69 also was described by the model, although the data are noisier (Fig. 4 *A*). This fit yielded a K_D of 1.4 ± 0.6 μM, and a K_X of $2.3 \pm 0.6 \times 10^{-4}$ per cell^{-1} (Table 1), values similar to those obtained

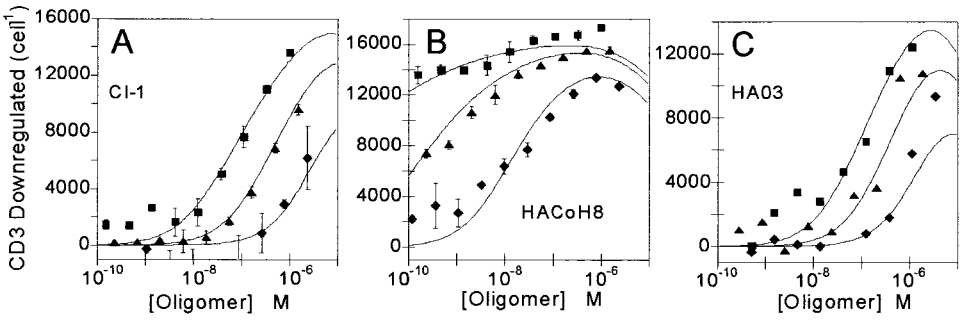

FIGURE 5 CD3 response in other T cells. These plots show the CD3 downregulation response to dimer (♦), trimer (▲), and tetramer (■) for the T cell clones (*A*) Cl-1 and (*B*) HACoH8 and for the (*C*) polyclonal cell line HA03. The smooth curves show the model fits for these data sets. Model parameters for these fits are shown in Table 2.

for CD3. If the CD3 downregulation and CD69 upregulation data are correlated, a linear relationship is seen with a slope of roughly 0.035 between the two (Fig. 4 *B*). This corresponds well with the ratio of the fit scale factors (0.027). Upregulation of CD25, the low-affinity IL-2 receptor, was not described well by the model using a linear scale factor (not shown). However, the plot of CD25 (IL-2R) upregulation versus CD3 downregulation did not exhibit a linear relationship as observed for CD69 with CD3, but rather a distinct curve (Fig. 4 *C*). A best-fit quadratic function was found for the relationship of CD3 and CD25, and that function was applied to the model predictions to better represent the behavior of the data. After this application, the CD25 upregulation data were fit well by the model (Fig. 4 *D*), giving best-fit values for K_D (1.8 ± 0.3 μM) and K_X (3.00 ± 0.01 per cell^{-1}) (Table 1). Again, these values were similar to those observed for the other markers.

Thus, a good correlation was observed between the predicted number of cross-linked receptors (R_{multi}) and the scaled experimental data ($R^2 = 0.99$) as shown in Figs. 3 and 4. We also fit each of the data sets using the number of cross-links (Φ_{xlink}), or the number of distinct dimers formed (R_{dimer}), instead of the number of cross-linked receptors. Although these fits were slightly less good (not shown), the experimental data are not sufficiently precise to be able to distinguish definitively between the different measures.

Analysis of other T-cell clones and MHC cross-linking strategies

Additional tests of this model were performed using two other influenza-specific T-cell clones, Cl-1 and HACoH8, and also a short-term polyclonal influenza-specific T-cell line raised from the peripheral blood of a DR1$^+$ homozygous individual, HA03 (Fig. 5). The dose–response of CD3 downregulation for the MHC oligomer series was measured for Cl-1 and HACoH8 after 24 hr (Fig. 5, *A* and *B*) and for HA03 after 12 hr (Fig. 5 *C*). For Cl-1, the CD3 downregulation dose–response curves were best-fit using $K_D = 5.00 \pm 0.01 \times 10^{-5}$ M and $K_X = 3.10 \pm 0.01 \times 10^{-4}$ per cell^{-1} (Table 2). These values are significantly different from those observed for HA1.7, particularly for K_D. The other T-cell clone, HACoH8, exhibited $K_D = 1.80 \pm 0.07 \times 10^{-6}$ M, and $K_X = 42.2 \pm 1.4 \times 10^{-4}$ per cell^{-1} (Table 2). In this case, the K_X value is substantially different from those observed for the other clones. Finally, the polyclonal line HA03 exhibited best-fit values of $K_D = 1.60 \pm 0.04 \times 10^{-5}$ M and $K_X = 0.96 \pm 0.04 \times 10^{-4}$ per cell^{-1} (Table 2). These data show that K_D and K_X values can vary among different T-cell lines, and that the model can describe these differences.

Another set of class II MHC oligomers has been used to investigate the effect of receptor proximity and orientation on T-cell activation (Cochran et al., 2001b). In this series, MHC dimers were linked using a direct disulfide bond between cysteines introduced at the end of the α or β subunit, or using peptide-based synthetic cross-linkers of varying length. Dimers linked through either the α or β subunits, using either a disulfide bond (S–S) or a long cross-linker (X14X), were tested for their ability to induce CD3 downregulation in the HA1.7 T-cell clone (Fig. 6). Dose–response curves for these dimers exhibited character-

TABLE 2 Comparison of binding parameters among different T cell clones*

T cell	R_{tot} (per cell)	K_D (μM)	K_X ($\times 10^{-4}$ cell)
HA1.7	24,000	1.70 (0.40)	3.15 (0.01)
Cl-1	16,700	60.00 (0.02)	3.10(0.01)
HACoH8	19,300	1.80 (0.07)	42.20 (1.4)
HA03†	27,000	16.00 (0.42)	0.96 (0.04)

*Parameters obtained by fitting CD3 downregulation data for HA1.7 (27 hrs), Cl-1 (24 hrs), HACoH8 (24 hrs), and HA03 (12 hrs). MHCs were linked through β subunit cysteines using peptide-based cross-linkers (Cochran et al., 2000). R_{tot} was measured directly by flow cytometry. Values in parentheses represent parameter uncertainties from the least squares fit (see Methods).
†Polyclonal T cell line.

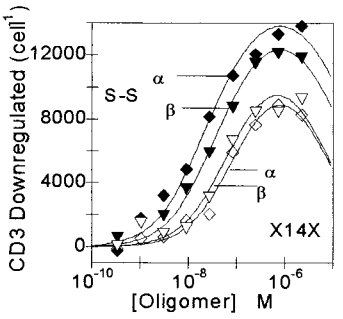

FIGURE 6 CD3 response to MHC dimers with different length cross-links. This plot shows the CD3 downregulation in response to directly disulfide-bonded S–S dimers linked through the α_{cys} (♦) or the β_{cys} (▼) cysteine, and X14X dimers connected by a long flexible linker between the α_{cys} (◇) or β_{cys} (▽) cysteine. The smooth lines show the model fit to the data. Best-fit parameters are shown in Table 3.

istic bell-shaped curves, with the S–S dimers (*closed symbols*) activating more potently than the X14X dimers (*open symbols*), with more activation induced at lower concentrations and a higher maximum response. The activation data were described well by the binding model (*lines*). Because the cross-linking site is remote from the peptide-binding region, the cross-links are not expected to interfere with the TCR interaction, and a single K_D value was globally fit to the curves. The K_X was allowed to vary between the curves. The K_D extracted from these curves (1.61 ± 0.31 μM) was consistent with other K_D values obtained for the HA1.7 T-cell clone. However, the best-fit K_X varied significantly within the series, with values (per cell)$^{-1}$ of $18.6 \pm 0.8 \times 10^{-4}$ (αS–S), $10.2 \pm 0.2 \times 10^{-4}$ (βS–S), $3.15 \pm 0.02 \times 10^{-4}$ (αX14X), and $3.79 \pm 0.03 \times 10^{-4}$ (βX14X) (Table 3). The K_X was greater for the S–S dimers, in which the MHC monomer units are positioned close together, and lower for the X14X dimers, which are more loosely tethered by the long, flexible linker. Thus, the K_X parameter appears to reflect more facile receptor cross-linking for the more compact dimers, as expected by their geometrical constraints.

TABLE 3 Comparison of K_X parameters obtained with differently linked MHC dimers*

MHC linkage†	Cross-linker Length‡ (Å)	K_X ($\times 10^{-4}$ cell)
S-S (α)	2	18.7 (0.8)
S-S (β)	2	10.2 (0.2)
X14X (α)	90	3.15 (0.02)
X14X (β)	90	3.78 (0.03)

*CD3 downregulation for HA1.7 at 20 hours. A single K_D value was globally fit to the data set as 1.6 μM. R_{tot} was measured at 21,300 per cell.
†MHCs were linked by disulfide bonds (S–S) or long peptide-based cross-linkers (X14X) through cystein residues on either the α or β subunit.
‡The length represents the predicted spacing of the linked $C\alpha$ atoms when the cross-linker is in an extended conformatioin.

Analysis of binding and competition data

In addition to the number of multivalently-bound receptors R_{multi}, the model can be used to predict the number of bound ligands, L_{bound}. This parameter is a sum over all of the variously bound states, and would be expected to correspond to the experimental ligand binding behavior. Figure 7, *A—C*, shows the predicted binding behavior for a series of oligomers of total valency 1 to 8, using values for K_D (1.4 μM) and K_X ($0.2–20 \times 10^{-4}$ cell^{-1}) similar to those observed experimentally (and identical to those of Fig. 2). For the lowest K_X value (2×10^{-5} cell^{-1}), the curves are closely spaced and similarly shaped, with slightly more shallow slope and closer spacing for the oligomers with increased valency (Fig. 7 *A*). At saturating concentration, distribution plots indicate that each oligomer is bound predominately monovalently (not shown). With a ten-fold increase in K_X, striking differences in shape are observed, with a strong asymmetry and greater spacing at lower oligomer concentrations as compared to the behavior at lower K_X (Fig. 7 *B*). At high concentration, the multivalent curves cross below the curve for monomeric binding. A high-valency oligomer will compete very effectively for binding sites relative to a monomeric ligand, and will occupy a given number of receptors using a smaller total number of bound oligomers (L_{bound}) as compared to a monomer. With another ten-fold increase in K_X (Fig. 7 *C*), this behavior is even more pronounced. Higher valency leads to a rapid rise in the number of oligomers bound at lower concentration, as seen by the wide spacing of the curves at low concentration. At higher concentration, the strength of the multivalent binding is a significant impediment to binding of additional oligomers, and increasing oligomer size results in fewer total oligomers bound as compared to smaller oligomers. Thus, the predicted binding behavior is very sensitive to the parameter K_X. Changes in the parameter K_D do not affect the shape of the curves, but simply shift them to different concentrations, with lower K_D resulting in a linear shift to lower concentrations (not shown). This is the same behavior as observed for the binding distribution plots (Fig. 2). As before, changes in R_{tot} resulted in changes identical to the corresponding change in K_X, but with changes in the saturation value.

Experimental oligomer binding data were described well by the model. Binding of the MHC oligomers can be measured concurrently with T-cell activation markers using fluorescent labels incorporated into the oligomer cross-linking reagents and multicolor flow cytometry (Cochran and Stern, 2000), although internalization of bound oligomer occurs during the extended incubations used for the activation assays (Cameron et al., 2001). The MHC oligomer series used earlier in the activation experiments was tested

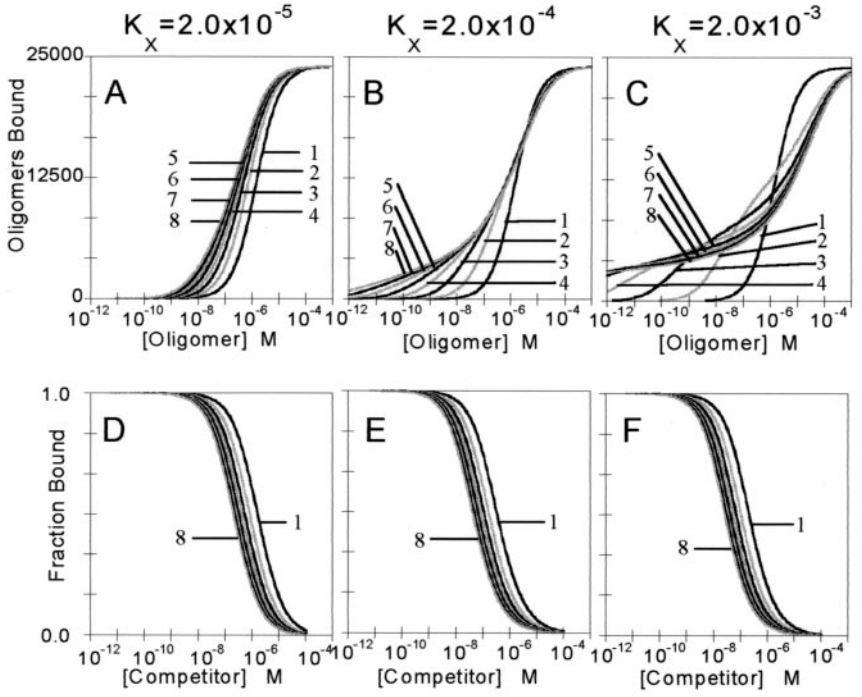

FIGURE 7 Simulation of binding and competition. (*A–C*) Direct binding of multivalent ligands to a cell surface in terms of number of oligomers bound, L_{bound}. Each curve shows the behavior of a given valency of oligomer binding to the cell. K_X increases as shown from panels (*A*) to (*C*). (*D–F*) Competition of a labeled tetramer (35 nM) by different valency unlabeled oligomers of the same ligand. K_X increases as shown from (*D*) to (*F*). R_{tot} = 24,000 per cell in all panels

for direct binding to the HA1.7 clone (Fig. 8). The experimental binding curves exhibit some of the characteristics of the predicted binding curves, including variable spacing depending on ligand concentration and convergence at high concentration (Fig. 8). These data were fit to the modeled total number of oligomers predicted to bind per cell at equilibrium (L_{bound}). The best fit to this data (Fig. 8) gives a K_D of 1.6 $\pm$ 0.3 μM and a K_X of 0.950 $\pm$ 0.001 $\times$ 10^{-4} per cell^{-1} (Table 1). These values are similar to the K_D and K_X values obtained independently from the T-cell activation data (Table 1). The scale factor from the direct binding fit was 0.806 $\pm$ 0.002, which is somewhat below unity perhaps because of partial quenching of the fluorescein labels in acidic compartments after endocytosis (Cameron et al., 2001).

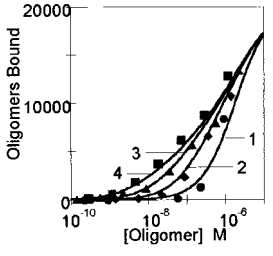

FIGURE 8 Direct binding data and fit. These curves show the experimental results for direct binding of labeled monomer (●), dimer (◆), trimer (▲), and tetramer (■) (Cochran et al., 2000), and the model fit to these data (*lines*). Parameters shown in Table 1.

The model can be used also to simulate competition experiments, in which a constant concentration of labeled "probe" oligomer is incubated in the presence of a variable concentration of unlabeled "competitor" oligomer or monomer. Figure 7, *D–F*, shows a series of predicted competition curves for oligomers of various valency, in each case using a constant concentration of probe tetramer (35 nM). These conditions are similar to those that have been used to evaluate relative oligomer binding (Cochran et al., 2000; Reichstetter et al., 2000). As before, three different values of K_X in the range of the experimental values are shown in Fig. 7, *D–F*, with each panel varying by a factor of ten from the adjacent panel. In contrast to the predicted binding curves, the shape of the competition curves are quite similar for oligomers of different valency, with only a small decrease in curve spacing with increasing valency. Moreover, changes in K_X result only in small shifts on the concentration axis rather than substantial changes in curve shape or spacing. A similar effect can be seen for changes of K_D. Thus, although the predicted curves fit well to experimental data (not shown), independent information about binding and cross-linking parameters cannot be extracted from this type of competition binding experiment.

DISCUSSION

We have applied a simple two-parameter binding model to the activation of antigen-specific T cells by oligomeric class II MHC proteins. We find that the model accurately describes important features of the T-cell responses to soluble MHC oligomers, including the bell-shaped, nonsaturating concentration dependence and the variation of response maxima with oligomer size. Similar dissociation constants (K_D) and cross-linking constants (K_X) were extracted from different assays, including direct oligomer binding data and measurement of the T-cell activation markers CD3 downregulation, CD69 upregulation, and CD25 upregulation, indicating that these parameters reflect intrinsic properties of the system. The strong correlation observed throughout the dose response between the levels of cellular activation and the predicted number of multivalently bound receptors suggests that these activation markers simply report the number of suitably engaged receptors. Elaborate multi-step cytoplasmic signaling pathways have been elucidated for T cell signaling pathways that lead to upregulation of gene expression, including receptor phosphorylation, assembly of multi-component signaling complexes on receptor cytoplasmic domains, activation of various tyrosine and serine/threonine kinase cascades, changes in intracellular Ca^{2+} concentration, and activation and nuclear translocation of transcription factors (Cantrell, 1996). The CD3 downregulation (receptor internalization) pathway is less completely understood, but appears to involve many of the same early processes (Itoh and Germain, 1997). Despite the apparent complexity of these signaling cascades, they do not appear to substantially modify the original binding signal, and the final cellular readout essentially reports the number of multivalently engaged receptors. For one marker (CD25), the relationship between binding and response was best described by a quadratic rather than linear relationship. Other activation responses may show other dependences and may incorporate information from other signaling pathways. Nonetheless, the simple correspondence between the number of engaged receptors and the degree of cellular activation observed many hours after stimulation is striking.

Implicit in the model is the notion that multivalent engagement of receptors leads to signaling, but that monovalent engagement does not. Although this is supported by recent experimental work, particularly in $CD4^+$ T cells (Boniface et al., 1998; Cochran et al., 2000), the biochemical basis of signal initiation is not yet clear. Receptor clustering is known to lead to phosphorylation of receptor cytoplasmic domains, but, currently, it is not clear how clustering results in kinase activation or in exposure of cytoplasmic domains, although several models have been proposed (Aivazian and Stern, 2000; Chan et al., 1994; Shaw and Dustin, 1997). The modeling performed here cannot definitively distinguish between a generic clustering mechanism where R_{multi} is the parameter that scales with T-cell activation, or a specific dimerization mechanism where R_{dimer} describes the triggering.

An individual's T-cell repertoire includes many different T-cell clones of varying MHC-TCR affinity and signaling capacity (Janeway et al, 2001). Moreover, a T cell in different developmental and activation states has different sensitivities to antigenic stimulation. Parameters derived from least-squares fitting of the model to experimental activation data can be used to understand and predict these functional differences among T cells. We applied the model to several different T-cell clones and to a polyclonal cell line representative of a subpopulation present in blood. The K_D and K_X parameters extracted from activation data differed for the different T cells, with the differences consistent with behavior observed in cellular assays. For example, the HACoH8 clone has a K_X value 13-fold higher than for HA1.7, indicating an increased tendency to form receptor cross-links. This clone can be stained by class II MHC oligomers even at 4°C, whereas most clones, including HA1.7 and Cl-1, require incubation at increased temperature to stain with those reagents (Cameron et al., 2001). The temperature dependence has been attributed to membrane or cytoskeletal rearrangements that are necessary for monomeric TCR to co-localize sufficiently to allow multivalent binding of MHC oligomers, and which are inhibited at low temperature (Cameron et al., 2001). The increased cross-linking tendency of HACoH8 would increase its ability to multivalently engage MHC oligomers, allowing oligomer staining under conditions where other clones are not stained.

With the increasing use of MHC tetramers in detection and analysis of specific T cells in clinical samples (McMichael and O'Callaghan, 1998), it is important to understand the parameters that govern the multivalent MHC-TCR interaction. Our analysis suggests that this relationship can be complex, with substantial nonlinear contributions from the receptor number (R_{tot}) and cross-linking propensity (K_X). In an early description of the use class II MHC oligomers, a linear correlation was observed between oligomer staining intensity and binding affinity K_D, for several T-cell hybridomas after correction for the total receptor number (Crawford et al., 1998). Our analysis suggests that this relationship will only hold for a restricted range of R_{tot}, and only for cells with similar K_X values. Finally, it is important to note that IC_{50} values determined from competition analysis cannot be related to MHC-TCR K_D values unless the relevant K_X values are known.

The sensitivity of the model to changes in K_X suggests a novel mechanism by which T cells could regulate their activation state. A naïve T cell, which has never previously seen antigen, is much more difficult to activate than the corresponding memory T cell, which is the long-lived product of a prior encounter to antigen (Janeway et al., 2001). Certain treatments with high antigen dose or with partial antigenic stimuli are known to "anergize" T cells, i.e., to drive them to nonantigen responsive state (Schwartz, 1997).

In both cases, the responsive and nonresponsive T cells express the same receptor, and so have the same MHC-TCR affinity. It has generally been thought that these changes in activation sensitivity are due to changes in the intracellular signaling pathways. However, it is possible that T cells could regulate their activity by changing their ability to cluster TCR in the plane of the membrane, without any change in cytoplasmic signaling processes. In our model, this would correspond to a change in K_X. Such changes could be effected by alteration of receptor-cytoskeletal interactions (Viola et al., 1999), by receptor localization to membrane raft microdomains (Xavier and Seed, 1999), or by alteration of the receptor oligomeric state (Fernandez-Miguel et al., 1999). Recently, differences in the binding avidity of naïve as compared to activated T cells have been observed, and attributed to differences in TCR oligomeric state (Fahmy et al., 2001); these could as well be due to differences in the dynamic cross-linking propensity rather than the static oligomeric state. The pronounced effects on ligand sensitivity that we have observed for relatively small changes in K_X (Figs. 2 and 5) suggest that substantial changes in activation potential can be realized without any change in the intracellular signaling pathways. In principle, this possible mechanism is similar to one hypothesized to regulate cellular sensitivity to soluble monomeric antigen through changes in receptor organization (Bray et al., 1998).

There are some shortcomings of this approach in modeling the activation of T cells. We assume that all cross-linking events are equivalent, but it is possible that sequential cross-linking interactions are governed by different K_X values. The model assumes a constant receptor number R_{tot}, although activated receptors become downregulated as part of the activation response (Liu et al., 2000), thus altering R_{tot} during the course of the experiment. We used the initial R_{tot} in calculating K_X values, because the T-cell response to soluble MHC oligomers is rapid (Boniface et al., 1998, and J. R. Cochran and L. J. Stern, unpublished results). Using the initial R_{tot}, similar K_X values were obtained at different times in the response with only a change in scale factor. However, for derivation of an actual thermodynamic association constant, a more sophisticated analysis might be warranted. Finally, because this is an equilibrium model, it does not account for kinetic features of the interaction that may play a role in triggering; for example, the off-rate of the MHC-TCR complex has been proposed to be more important in regulating activation behavior than the affinity (Matsui et al., 1994).

Despite the simplifications made by the model, it correctly predicts T-cell binding and activation behavior within observed experimental error. This model should prove useful in guiding experimental detection of T cells using MHC oligomers, and it provides a quantifiable measure of cellular parameters that appear to regulate antigen sensitivity in T cells.

We thank Corinne Moulon for the HACoH8 clone, A. Sette for Cl-1, J. Lamb for HA1.7, and Bader Yassine-Diab and Tom Cameron for providing the HA03 polyclonal line.

This work was supported by National Institutes of Health grant NO1-AI48833 (L.J.S.) and a National Institutes of Health Biotechnology Training grant NIH-T32-GM08334 (J.D.S., J.R.C.).

REFERENCES

Abastado, J. P., Y. C. Lone, A. Casrouge, G. Boulot, and P. Kourilsky. 1995. Dimerization of soluble major histocompatibility complex-peptide complexes is sufficient for activation of T cell hybridoma and induction of unresponsiveness. *J. Exp. Med.* 182:439–447.

Aivazian, D. A., and L. J. Stern. 2000. Phosphorylation of T cell receptor zeta is regulated by a lipid dependent folding transition. *Nat. Struct. Biol.* 7:1023–1026.

Appel, H., L. Gauthier, J. Pyrdol, and K. W. Wucherpfennig. 2000. Kinetics of T-cell receptor binding by bivalent HLA-DR.Peptide complexes that activate antigen-specific human T-cells. *J. Biol. Chem.* 275:312–321.

Bevington, P. R. 1969. Data Reduction and Error Analysis for the Physical Sciences. McGraw-Hill Book Company, New York. 242–245.

Boniface, J. J., J. D. Rabinowitz, C. Wulfing, J. Hampl, Z. Reich, J. D. Altman, R. M. Kantor, C. Beeson, H. M. McConnell, and M. M. Davis. 1998. Initiation of signal transduction through the T cell receptor requires the multivalent engagement of peptide/MHC ligands. *Immunity.* 9:459–466.

Bray, D., M. D. Levin, and C. J. Morton-Firth. 1998. Receptor clustering as a cellular mechanism to control sensitivity. *Nature.* 393:85–88.

Cameron, T. O., J. R. Cochran, B. Yassine-Diab, R.-P. Sekaly, and L. J. Stern. 2001. Detection of antigen-specific CD4+ T cells by HLA-DR1 oligomers in dependent on an active cellular process. *J. Immunol.* 166: 741–745.

Cantrell, D. 1996. T cell antigen receptor signal transduction pathways. *Annu. Rev. Immunol.* 14:259–274.

Casares, S., C. S. Zong, D. L. Radu, A. Miller, C. A. Bona, and T. D. Brumeanu. 1999. Antigen-specific signaling by a soluble, dimeric peptide/major histocompatibility complex class II/Fc chimera leading to T helper cell type 2 differentiation. *J. Exp. Med.* 190:543–553.

Chambers, C. A. 2001. The expanding world of co-stimulation: the two-signal model revisited. *Trends Immunol.* 22:217–223.

Chan, A. C., D. M. Desai, and A. Weiss. 1994. The role of protein tyrosine kinases and protein tyrosine phosphatases in T cell antigen receptor signal transduction. *Annu. Rev. Immunol.* 12:555–592.

Chicz, R. M., R. G. Urban, W. S. Lane, J. C. Gorga, L. J. Stern, D. A. A. Vignali, and J. L. Strominger. 1992. Predominant naturally processed peptides bound to HLA-DR1 are derived from MHC-related molecules and are heterogeneous in size. *Nature.* 358:764–768.

Cochran, J. R., D. Aivazian, T. O. Cameron, and L. J. Stern. 2001a. Receptor clustering and transmembrane signaling in T cells. *Trends Biochem. Sci.* 26:304–310.

Cochran, J. R., T. O. Cameron, and L. J. Stern. 2000. The relationship of MHC-peptide binding and T cell activation probed using chemically defined MHC class II oligomers. *Immunity.* 12:241–250.

Cochran, J. R., T. O. Cameron, J. D. Stone, J. B. Lubetsky, and L. J. Stern. 2001b. Receptor proximity, not intermolecular orientation, is critical for triggering T-cell activation. *J. Biol. Chem.* 276:28068–28074.

Cochran, J. R., and L. J. Stern. 2000. A diverse set of oligomeric class II MHC-peptide complexes for probing T-cell receptor interactions. *Chem. Biol.* 7:683–696.

Crawford, F., H. Kozono, J. White, P. Marrack, and J. Kappler. 1998. Detection of antigen-specific T cells with multivalent soluble class II MHC covalent peptide complexes. *Immunity.* 8:675–682.

Davis, M. M., J. J. Boniface, Z. Reich, D. Lyons, J. Hampl, B. Arden, and Y. Chien. 1998. Ligand recognition by alpha beta T cell receptors. *Annu. Rev. Immunol.* 16:523–544.

DeLisi, C., and R. Chabay. 1979. The influence of cell surface receptor clustering on the thermodynamics of ligand binding and the kinetics of dissociation. *Cell Biophys.* 1:117–131.

DeLisi, C., and R. Siraganian. 1979. Receptor cross-linking and histamine release II. Interpretation and analysis of anomalous dose response patterns. *J. Immunol.* 122:2293–2299.

Fahmy, T. M., J. G. Bieler, M. Edidin, and J. P. Schneck. 2001. Increased TCR avidity after T cell activation: a mechanism for sensing low-density antigen. *Immunity.* 14:135–143.

Ferlin, W., N. Glaichenhaus, and E. Mougneau. 2000. Present difficulties and future promise of MHC multimers in autoimmune exploration. *Curr. Opin. Immunol.* 12:670–675.

Fernandez-Miguel, G., B. Alarcon, A. Iglesias, H. Bluethmann, M. Alvarez-Mon, E. Sanz, and A. de la Hera. 1999. Multivalent structure of an alphabetaT cell receptor. *Proc. Natl. Acad. Sci. U.S.A.* 96:1547–1552.

Frayser, M., A. K. Sato, L. Xu, and L. J. Stern. 1999. Empty and peptide-loaded class II major histocompatibiliby complex proteins produced by expression in *Escherichia coli* and folding in vitro. *Protein Expr. Purif.* 15:105–114.

Germain, R. N. 1994. MHC-dependent antigen processing and peptide presentation: providing ligands for T lymphocyte activation. *Cell.* 76: 287–299.

Germain, R. N. 1997. T-cell signaling: the importance of receptor clustering. *Curr. Biol.* 7:R640–R644.

Hamad, A. R., S. M. O'Herrin, M. S. Lebowitz, A. Srikrishnan, J. Bieler, J. Schneck, and D. Pardoll. 1998. Potent T cell activation with dimeric peptide-major histocompatibility complex class II ligand: the role of CD4 coreceptor. *J. Exp. Med.* 188:1633–1640.

Hlavacek, W. S., A. S. Perelson, B. Sulzer, J. Bold, J. Paar, W. Gorman, and R. G. Posner. 1999. Quantifying aggregation of IgE-FcϵRI by multivalent antigen. *Biophys. J.* 76:2421–2431.

Irving, B. A., and A. Weiss. 1991. The cytoplasmic domain of the T cell receptor zeta chain is sufficient to couple to receptor-associated signal transduction pathways. *Cell.* 64:891–901.

Itoh, Y., and R. N. Germain. 1997. Single cell analysis reveals regulated hierarchical T cell antigen receptor signaling thresholds and intraclonal heterogeneity for individual cytokine responses of CD4+ T cells. *J. Exp. Med.* 186:757–766.

Janeway, C. A. 1995. Ligands for the T-cell receptor: hard times for avidity models. *Immunol. Today.* 16:223–225.

Janeway, C. A., P. Travers, M. Walport, and M. Shlomchik, 2001. Immunobiology: The Immune System in Health and Disease, chapter 8. Garland Publishing Inc, New York.

Kreyszig, E. 1993. Numerical methods. *In* Advanced Engineering Mathematics. J. Carrafiello, editor. John Wiley and Sons, Inc., New York. 916–1082.

Lamb, J. R., D. D. Eckels, P. Lake, J. N. Woody, and N. Green. 1982. Human T-cell clones recognize chemically synthesized peptides of influenza haemagglutinin. *Nature.* 300:66–69.

Letourneur, F., and R. D. Klausner. 1991. T-cell and basophil activation through the cytoplasmic tail of T-cell- receptor zeta family proteins. *Proc. Natl. Acad. Sci. U.S.A.* 88:8905–8909.

Liu, H., M. Rhodes, D. L. Wiest, and D. A. A. Vignali. 2000. On the dynamics of TCR:CD3 complex cell surface expression and downmodulation. *Immunity.* 13:665–675.

Matsui, K., J. J. Boniface, P. Steffner, P. A. Reay, and M. M. Davis. 1994. Kinetics of T-cell receptor binding to peptide/I-E^k complexes: correlation of the dissociation rate with T-cell responsiveness. *Proc. Natl. Acad. Sci. U.S.A.* 91:12862–12866.

McMichael, A. J., and C. A. O'Callaghan. 1998. A new look at T cells. *J. Exp. Med.* 187:1367–1371.

Perelson, A. S. 1981. Receptor clustering on a cell surface. III. Theory of receptor cross-linking by multivalent ligands: Description by ligand states. *Math. Biosci.* 53:1–39.

Qian, D., and A. Weiss. 1997. T cell antigen receptor signal transduction. *Curr. Opin. Cell Biol.* 9:205–212.

Reichstetter, S., R. A. Ettinger, A. W. Liu, J. A. Gebe, G. T. Nepom, and W. W. Kwok. 2000. Distinct T cell interactions with HLA class II tetramers characterize a spectrum of TCR affinities in the human antigen-specific T cell response. *J. Immunol.* 165:6994–6998.

Schwartz, R. H. 1997. T cell clonal anergy. *Curr. Opin. Immunol.* 9:351–357.

Sette, A., J. Alexander, J. Ruppert, K. Snoke, A. Franco, G. Ishioka, and H. Grey. 1994. Antigen analogs/MHC complexes as specific T cell receptor antagonists. *Annu. Rev. Immunol.* 12:413–431.

Shaw, A. S., and M. L. Dustin. 1997. Making the T cell receptor go the distance: a topological view of T cell activation. *Immunity.* 6:361–369.

Testi, R., D. D'Ambrosio, R. De Maria, and A. Santoni. 1994. The CD69 receptor: a multipurpose cell-surface trigger for hematopoietic cells. *Immunol. Today.* 15:479–483.

Valitutti, S., S. Muller, M. Salio, and A. Lanzavecchia. 1997. Degradation of T cell receptor (TCR)-CD3-ζ complexes after antigenic stimulation. *J. Exp. Med.* 185:1859–1864.

van der Merwe, P. A., S. J. Davis, A. S. Shaw, and M. L. Dustin. 2000. Cytoskeletal polarization and redistribution of cell-surface molecules during T cell antigen recognition. *Semin. Immunol.* 12:5–21.

Viola, A., S. Schroeder, Y. Sakakibara, and A. Lanzavecchia. 1999. T lymphocyte costimulation mediated by reorganization of membrane microdomains. *Science.* 283:680–682.

Waldmann, T. A. 1989. The multi-subunit interleukin-2 receptor. *Annu. Rev. Biochem.* 58:875–911.

Wickham, T. J., R. R. Granados, H. A. Wood, D. A. Hammer, and M. L. Shuler. 1990. General analysis of receptor-mediated viral attachment to cell surfaces. *Biophys. J.* 58:1501–1516.

Xavier, R., and B. Seed. 1999. Membrane compartmentation and the response to antigen. *Curr. Opin. Immunol.* 11:265–269.